



## Supplementary Materials for

### **Developing a pro-regenerative biomaterial scaffold microenvironment requires T helper 2 cells**

Kaitlyn Sadtler, Kenneth Estrellas, Brian W. Allen, Matthew T. Wolf, Hongni Fan, Ada J. Tam, Chirag Patel, Brandon S. Lubber, Hao Wang, Kathryn R. Wagner, Jonathan D. Powell, Franck Housseau, Drew M. Pardoll, Jennifer H. Elisseeff\*

\*Corresponding author. E-mail: [jhe@jhu.edu](mailto:jhe@jhu.edu)

Published 15 April 2016, *Science* **352**, 366 (2016)  
DOI: 10.1126/science.aad9272

#### **This PDF file includes:**

Materials and Methods  
Figs. S1 to S14  
Tables S1 and S2  
References (34, 35)

## MATERIALS AND METHODS

### Tissue ECM Selection and Preparation

Porcine derived tissues (Wagner Meats, Mt. Airy MD) were processed following a standard protocol. Samples were formulated into a paste through the use of a knife-mill processor (Retsch, Germany) with particle sizes no larger than 5 mm<sup>2</sup> and rinsed thoroughly with running distilled water until blood was cleared from samples. Bone samples were pre-treated for decalcification by incubation in 10% formic acid (Sigma) for 3 days, which was verified by a colorimetric calcium test (STANBIO Laboratory). Tissues were then incubated in 3.0% peracetic acid (Sigma) on a shaker at 37°C for 4 hours, with a change to fresh acid solution after 1 hour. pH was adjusted to 7 with thorough water and PBS rinsing, and tested after solution was freshly changed and tissue rested for 20 minutes. Samples were washed once more with distilled water then transferred to a 1% Triton-X100 (Sigma) + 2 mM sodium EDTA (Sigma) solution on a stir plate at 400 rpm, room temperature for 3 days, changing the solution daily. Tissues were rinsed thoroughly with distilled water until no bubbles formed from detergent upon agitation. Finally, processed tissues were incubated in 600 U/ml DNase I (Roche Diagnostics) + 10 mM MgCl<sub>2</sub> (J. T. Baker) + 10% Antifungal-Antimycotic (Gibco®) for 24 hours. Tissues were rinsed thoroughly with distilled water, then frozen at -80°C and lyophilized for 3 days. The dry sample was turned into a particulate form using a SPEX SamplePrep Freezer/Mill (SPEX CertiPrep). ECM powder was stored between -20°C and -80°C and UV sterilized prior to use. Collagen from bovine tendon (Sigma) was cryomilled using the SPEX SamplePrep Freezer/Mill to form a particulate similar to the whole tissue ECM samples. This would serve as the “single-component” control for the studies compared to tissue-derived complex ECM scaffolds.

Broad tissue ECM source screening for macrophage response was previously performed using a tissue array and cell morphological analysis (1). A focused screen of 5 tissues (lung, cardiac, bone, spleen, and liver) was then performed in vitro to evaluate macrophage M1 (CD86) and M2 (CD 206) marker expression (as described in detail in the cell culture and in vitro flow cytometry methods). These tissues were selected for the focused screen due to the range of morphological results in the previously referenced publication (13) and also the desire to include a sampling of tissue properties (highly cellular tissues versus dense connective tissues). For translation to the in vivo traumatic wound model, cardiac and bone tissue was selected due to their diverse response in M1 and M2 markers FACS and their varying proteomic composition (cellular non ECM components versus a connective tissue with primarily ECM components, respectively). Furthermore, a clinically used material (Matristem, urinary bladder matrix) was tested to compare in vivo CD86 levels.

## Cell Culture

Murine immortalized bone marrow macrophages (iBMM, (34)) were cultured as per developer's protocol in IMDM (Gibco®) media containing 20% FBS (Hyclone, GE Healthcare Life Sciences), 2.5 mM L-glutamine (Gibco®), 1% PenStrep (Life Technologies), and 50 ng/ml M-CSF (Recombinant Mouse, BioLegend). iBMM cells were compared to primary (BMDMs) cells using RT-PCR after 24 hours of polarization in conditioned media (M0, M1, or M2 media) and confirmed to be a reliable *in vitro* comparison to primary macrophages (Fig. S1). Specifically, iBMM macrophages were cultured on plates coated with ECM powder for 24 hours in growth medium, or medium supplemented with 200 ng/ml *E. coli* lipopolysaccharide (LPS 055:B5, Sigma) and 20 ng/ml interferon gamma (IFN $\gamma$ , Peprotech) or 20 ng/ml interleukin-4 (IL-4, Peprotech), for M1 and M2 polarizations, respectively. Prior to cell seeding, ECM powder was resuspended to 4-5 mg/ml in distilled water, and coated (1 ml/well) on 6-well plates by allowing the solution to air dry. After dry, plates were sterilized under UV and rinsed with 1XPBS directly before cell seeding to remove non-adhered particles. iBMM macrophages performed similarly to BMDM in gene expression studies (upregulating *Tnfa* *I11b* and *Inos* in M1 conditions, and *Arg1* and *Retnla* in M2 conditions). Additionally they adopted characteristic morphological changes and expressed CD86 during M1 stimulation and CD206 during M2 stimulation (see Flow Cytometry: *In vitro* screening section for more detail).

## Flow Cytometry: *In vitro* screening

*In vitro* samples were harvested using Accutase (Life Technologies) and washed with cold 1X PBS. Then, cells were stained with the following antibody panel: F4/80 PE-Cy7 (BioLegend), CD11b Pacific Blue (BioLegend), CD11c APC-Cy7 (BD Biosciences), CD86 AlexaFluor700 (BioLegend), MHCII (I-A/I-E) AlexaFluor488 (BioLegend), CD206 APC (BioLegend) and LIVE/DEAD® Fixable Aqua Dead Cell Stain Kit (Life Technologies). Samples were fixed using the BD Cytotfix/Cytoperm™ kit (BD Biosciences), and run on BD LSRII Cell Analyzer, data was analyzed using FlowJo Flow Cytometry Analysis Software (Treestar). M1/M2 polarization levels were determined by mean fluorescence intensity of CD86 and CD206 in LIVE/DEAD® Fixable Aqua Dead Cell Stain F4/80<sup>+</sup>CD11c<sup>-</sup> cells.

## Volumetric Muscle Loss (VML) Surgery

Six- to eight-week-old female wild type C57BL/6 (Charles River), B6.129S7-*Rag1*<sup>tm1Mom</sup>/J, BALB/c-*Il4ra*<sup>tm1Sz</sup>/J, or B6.129S2-*Cd4*<sup>tm1Mak</sup>/J (Jackson Laboratories) mice were anesthetized with 4.0% isoflurane and maintained under 2.5% isoflurane. Hair was removed from the lower extremities with an electric razor (Oster). After ethanol sterilization of the surrounding skin, a 1.5-cm incision was created between the knee and

hip joint to access the quadriceps femoris muscle. Through the use of surgical scissors, a 3 mm x 3 mm deep defect was created in the quadriceps femoris muscle group. The resulting bilateral defects were filled with 0.05 cc of a 200 - 300 mg/ml biomaterial scaffold (UV-sterilized ECM (manufactured in house) or Collagen (Sigma)) or 0.05 cc of a vehicle (saline) control. Mice were under anesthesia for 10 – 15 minutes during surgical preparation and procedure before return to cage and monitored until ambulatory. Directly after surgery, mice were given subcutaneous carprofen (Rimadyl®, Zoetis) at 5 mg/kg for pain relief and were maintained on Uniprim® antibiotic feed (275 ppm Trimethoprim and 1365 ppm Sulfadiazine, Harlan Laboratories) until the end of study to prevent opportunistic infections. After 1 (7 days), 3 (24 days) and 6 (42 days) weeks, the mice were sacrificed and their entire quadriceps femoris muscle was removed by cutting from the knee joint along the femur to the hip joint. Both inguinal and axillary/brachial lymph nodes and whole muscle samples for RNA isolation were flash frozen in liquid nitrogen and stored at -80°C until RNA extraction. All animal procedures in this study were conducted in accordance with an approved Johns Hopkins University IACUC protocol.

### **T cell Adoptive Transfer**

CD4<sup>+</sup> T cells were isolated from lymph nodes and spleens of wild type C57BL/6 and B6.*Rictor*<sup>-/-</sup> mice (a gift from Jonathan Powell, created by crossing B6.*Rictor*<sup>F/F</sup> with B6.Cd4-cre) using MACS CD4<sup>+</sup> T Cell Isolation Kit (Miltenyi Biotec) as per manufacturers instructions. Purity was confirmed by staining with the following FACS antibody panel: CD3 AlexaFluor488, CD4 PE-Cy7, CD8 APC (Biolegend). Three million CD4<sup>+</sup> T cells were injected into B6.129S7-*Rag1*<sup>tm1Mom</sup>/J. After 12 days post-injection, mice were tested for T cell presence and CD4/CD8 purity in peripheral blood to confirm repopulation. After 2 weeks, muscle surgery was performed as per previously described.

### **RT-PCR**

*In vivo* inguinal and axillary/brachial lymph node samples from volumetric muscle loss (VML) studies were homogenized in TRIzol and RNA was extracted using a combination of TRIzol and RNeasy Mini (Qiagen) column-based isolations. cDNA was synthesized through the use of SuperScript Reverse Transcriptase III (Life Technologies) as per manufacturer's instructions. RT-PCR was conducted on an Applied Biosystems Real Time PCR Machine using SYBR Green (Life Technologies) as a reporter and the following primers: *B2m* forward CTC GGT GAC CCT GGT CTT TC, *B2m* reverse GGA TTT CAA TGT GAG GCG GG; *Tnfa* forward GTC CAT TCC TGA GTT CTG, *Tnfa* reverse GAA AGG TCT GAA GGT AGG; *Il1β* forward GTA TGG GCT GGA CTG TTT C, *Il1β* reverse GCT GTC TGC TCA TTC ACG; *Retnla* forward CTT TCC TGA GAT TCT GCC CCA G, *Retnla* reverse CAC AAG CAC ACC CAG TAG CA; *Ifny* forward TCA AGT GGC ATA GAT GTG GAA, *Ifny* reverse TGA GGT AGA AAG

AGA TAA TCT GG; *Il4* forward ACA GGA GAA GGG ACG CCA T, *Il4* reverse ACC TTG GAA GCC CTA CAG A. Whole muscle samples were processed similarly to lymph nodes to isolate RNA and produce cDNA. Primers used included those previously described and: *Arg1* forward CAG AAG AAT GGA AGA GTC AG, *Arg1* reverse CAG ATA TGC AGG GAG TCA CC; *Coll1a1* forward CTG GCG GTT CAG GTC CAA T, *Coll1a1* reverse TTC CAG GCA ATC CAC GAG C; *Fabp4* forward TCA CCT GGA AGA CAG CTC CT, *Fabp4* reverse AAT CCC CAT TTA CGC TGA TG; *AdipoQ* forward TCC TGG AGA GAA GGG AGA GAA AG, *AdipoQ* reverse TCA GCT CCT GTC ATT CCA ACA T; *Lep* forward TTC ACA CAC GCA GTC GGT AT, *Lep* reverse ACA TTT TGG GAA GGC AGG CT; *Actb* forward ATG TGG ATC AGC AAG CAG GA, *Actb* reverse AAG GGT GTA AAA CGC AGC TCA (Integrated DNA Technologies). F4/80<sup>+</sup> and CD3<sup>+</sup> cells from volumetric muscle wounds were sorted directly into RNA lysis buffer; RLT buffer (Qiagen) +  $\beta$ -mercaptoethanol (Sigma). RNA was isolated using an RNeasy Micro Kit (Qiagen) with carrier RNA and on-column DNase treatment. cDNA synthesis was performed with a High Capacity cDNA Reverse Transcription Kit (Applied Biosystems). Isolated RNA underwent preamplification prior to plating in custom 96-well TaqMan<sup>®</sup> Array Fast Plates (Life Technologies) and gene expression was detected on an Applied Biosystems StepOne Real-Time PCR System.

### **Histology**

Inguinal lymph nodes were harvested and fixed in formalin overnight before dehydration and paraffin embedding, microtome sectioning, then histological examination via hematoxylin and eosin staining. Muscle samples were prepared as fresh-frozen samples for cryosectioning by flash freezing in isopentane after mounting in Tragacanth gum (Sigma Life Science). A Microm HM 550 cryostat (Fisher Scientific) was used to obtain 10  $\mu$ m cryosections from 5-7 different regions of each muscle roughly 300  $\mu$ m apart. Sections were stained with a Hematoxylin and Eosin protocol (Sigma Aldrich) or with a Modified Masson's Trichrome protocol.

### **Flow Cytometry**

Muscle wounds and surrounding area were harvested at 1 (7 days), 3 (24 days) and 6 (42 days) weeks post-surgery by cutting the quadriceps muscle from the hip to the knee and finely diced in 1X PBS. Resultant material was digested for 45 minutes at 37°C in 1.67 Wunsch U/ml Liberase TL (Roche Diagnostics) + 0.2 mg/ml DNase I (Roche Diagnostics) in serum-free RPMI-1640 medium (Gibco) on a shaker at 400 rpm. Digest was filtered through a 100  $\mu$ m cell strainer (Fisher) then washed twice with 1X PBS. Cells were resuspended in 5 ml 1X PBS and layered atop 5 ml Lympholyte-M (Cedarlane), then spun for 20 minutes at 1200 x g. Cellular interphase was washed twice with 1X PBS. Isolated cells were stained with the following antibody panel: LIVE/DEAD<sup>®</sup> Fixable Aqua Dead Cell Stain Kit (Life Technologies), CD19

BrilliantViolet 421 (BioLegend), CD3 AlexaFluor 488 (BioLegend), CD11c APC-Cy7 (BD Biosciences), F4/80 PE-Cy7 (BioLegend), CD86 AlexaFluor700 (BioLegend), CD206 APC (BioLegend). After staining cells were fixed and analyzed on a BD LSR Analyzer (BD Biosciences). LIVE/DEAD® Fixable Aqua Dead Cell Stain negative (live) cells were evaluated based upon percent population of T cells (CD3<sup>+</sup>), B cells (CD19<sup>+</sup>), dendritic cells (CD11c<sup>+</sup>), and macrophages (F4/80<sup>+</sup>). Macrophages were further analyzed for polarization by mean fluorescence intensity of F4/80<sup>+</sup>, CD11c<sup>+</sup> and F4/80<sup>+</sup>CD11c<sup>+</sup> cells in CD86 AlexaFluor700 and CD206 APC channels. All analyses were performed in FlowJo Flow Cytometry Analysis Software (Treestar). The T cell panel included: LIVE/DEAD® Fixable Aqua Dead Cell Stain Kit (Life Technologies), CD3 AlexaFluor488 (BioLegend), CD4 PE-Cy7 (BioLegend), CD8 AlexaFluor 700 (BioLegend), FoxP3 Pacific Blue (BioLegend), IL4ra PE (BioLegend) and CCR5 APC (BioLegend). FoxP3 staining followed fixation and permeabilization with BD CytoFix/CytoPerm Kit (BD Biosciences). Samples prepared for sorting of F4/80<sup>+</sup> and CD3<sup>+</sup> cells followed the same isolation, then were stained with Fixable Viability Dye eFluor®780 (eBioscience), F4/80 PE-Cy7 (BioLegend), CD11c APC-Cy7 (BD Biosciences) and CD3 AlexaFluor488 (BioLegend). Samples were run on a BD FACS Aria and collected directly into RLT lysis buffer (Qiagen) containing β-mercaptoethanol (Sigma), and stored at -80<sup>o</sup>C until RNA isolation.

### Statistical Analysis

All samples are representative of  $n = 4$  mice and are representative of at least 2 independent experiments unless otherwise stated. Data are displayed as mean  $\pm$  standard error of the mean. Statistical outliers were removed using Grubbs' outlier test at alpha = 0.05 using GraphPad Prism v6 Software (GraphPad Software Inc., La Jolla, CA). Two-way ANOVAs were performed (GraphPad Prismv6), with statistical significance designated at  $p \leq 0.05$ . For multiple comparisons, Tukey or Dunnet post-test corrections were applied. For gene expression analyses of sorted CD3<sup>+</sup>, F4/80<sup>+</sup> WT, and F4/80<sup>+</sup> *Rag1*<sup>-/-</sup> cells, scatter plots, heat maps, and correlation matrices of gene expression levels were used to compare across different materials: Saline, Bone, Cardiac, Collagen. To distinguish which groups of genes were differentially expressed based on material vs. saline, we used a re-sampling based permutation test based on the maximum Wilcoxon Rank Sum statistic within the gene group. Individual gene expression was also compared across material and saline using the Wilcoxon Rank Sum test. We compare expression between F4/80 WT and *Rag1*<sup>-/-</sup> for each material using the Wilcoxon Rank Sum test. We compare the difference of each material and saline between F4/80 WT and *Rag1*<sup>-/-</sup> using linear regression models (material by *Rag1*<sup>-/-</sup>-status interaction). Due to the exploratory nature and the small sample size, adjustment for multiple comparisons was not considered. Statistical analyses were performed using the R statistical package (version 2.15.1). Power analysis was not conducted to determine sample size.

### **Micro-CT Imaging**

Imaging was conducted using the Sedecal SuperArgus 4R PET/CT system. We acquired 720 projection images over 360 degrees in 0.5 degree increments; the maximum resolution mode was used, which means each acquired projection image is magnified 5.5 times when compared with the object. The x-ray tube was set with 50 kVp and 100  $\mu$ A. Exposure time for each projection was 350 ms. Projection images were stored in a matrix with dimensions 1536x972, with 0.15 mm pixel size. CT images were reconstructed using Cobra reconstruction software. Each CT image was stored in a matrix with size 1344x1344x864 with voxel size 0.031 mm. Each image in figure was contrast-enhanced to show defects, the same enhancements were applied for each image.

### **Treadmill Testing for Muscle Function**

Forty-eight hours prior to testing, mice were trained on treadmill apparatus running at 5 m/min and increased by 1 m/min every minute for a total of 5 minutes. Mice were run to exhaustion starting at 5 m/min and increased by 1 m/min every minute. Exhaustion was defined as when the mouse stayed on the pulsed shock grid for a continuous 30 seconds (Treat NMD). Animals were tested at least 48 hours prior to harvesting for analysis via FACS, PCR, or histology.

### **AUTHOR CONTRIBUTIONS**

K.S. conceived the study, designed experiments and wrote the manuscript. K.S., K.E., B.W.A., and H.F. performed experiments. K.S., K.E., and M.T.W performed muscle surgeries and data analysis. A.J.T. assisted on flow cytometric analyses. C.P. performed the adoptive transfers into immunodeficient mice and aided in mTOR studies. B.S.L. and H.W. performed statistical analyses of sorted cell gene expression studies. K.R.W. provided functional testing equipment and guidance in muscle surgical procedures and study design. J.D.P. provided guidance on mTOR mechanism and adoptive transfer experiments and provided the Rictor<sup>F/F</sup>-Cd4-Cre mouse line. F.H., D.M.P., and J.H.E. designed experiments, analyzed data and wrote the manuscript. D.M.P. and J.H.E. conceived the study and oversaw all experiments.

## SUPPLEMENTAL FIGURES

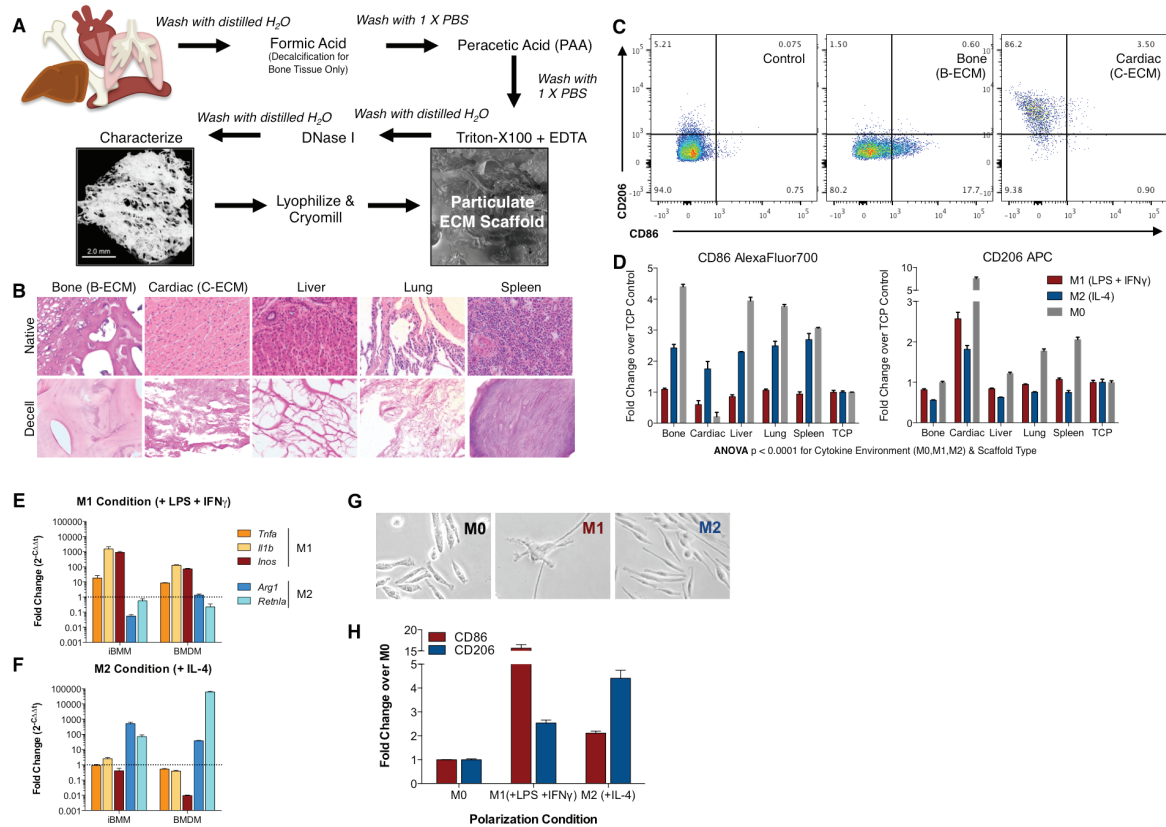


**Fig. S1: Materials characterization and selection.** (A) Extracellular matrix (ECM) scaffold preparation. (B) Histological staining (hematoxylin & eosin) of tissues pre- and post- ECM processing, top row = native cellular tissue (Native), bottom row = isolated extracellular matrix (Decell). (C-D) In vitro flow cytometric analysis of iBMM (immortalized bone marrow macrophage; Squadrito et. al. 2014) cell line cultured on varying ECM substrates identifies Bone (B-ECM) and Cardiac (C-ECM) as strong immunomodulatory scaffolds. CD86 = type-1 inflammatory macrophage, CD206 = type-2 alternative macrophage. (E-H) Verification of iBMM cell line. (E-F) qRT-PCR comparing gene expression between iBMM and primary bone-marrow derived macrophages (BMDM) in control M1 (E, LPS + IFN $\gamma$ ) and M2 (F, + IL-4) media conditions. *Tnfa*, *Il1b*, *Inos* = M1 markers. *Arg1*, *Retnla* = M2 markers. (G) Morphological characterization of iBMM in M0, M1 and M2 media conditions. (H) Flow cytometric analysis of iBMM in control polarizing conditions. Data in (D & H) are expressed as fold change over TCP control in the corresponding media condition (M1, M2, or M0). (E-F) are expressed as fold change over gene expression ( $2^{-\Delta\Delta C_t}$ ) in M0 unstimulated growth media. Data are means  $\pm$  SEM  $n = 3$ .

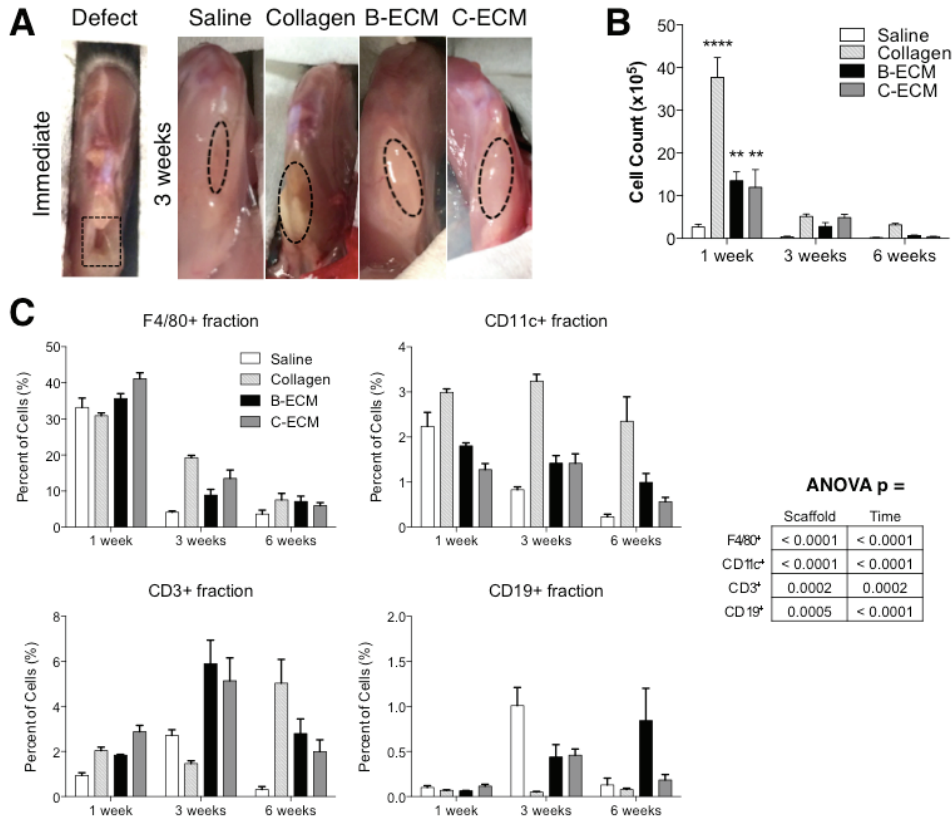


**Fig. S2: Cell recruitment to muscle injury.** (A) Gross images of mouse quadriceps muscle at 3 weeks post-operation. (B) Total number of cells infiltrating Saline- and scaffold-treated wounds. (C) Percent of overall cell population identified as F4/80<sup>+</sup> macrophages, CD11c<sup>+</sup> dendritic cells, CD3<sup>+</sup> T cells or CD19<sup>+</sup> B cells. Data are means  $\pm$  SEM  $n = 4$ .

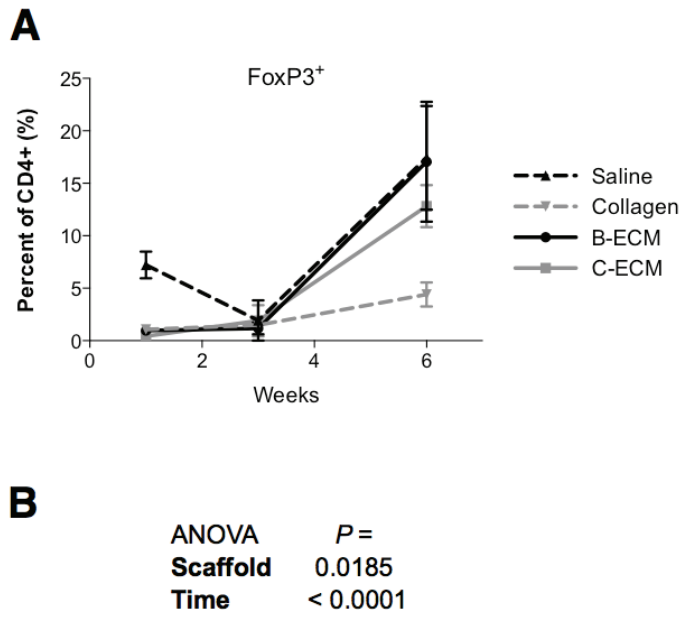


**Fig. S3: FoxP3<sup>+</sup> T<sub>reg</sub> populations at 1 and 3 weeks post-operation.** (A) Proportion of FoxP3<sup>+</sup>CD4<sup>+</sup> T cells in the defect at 1, 3, and 6 weeks post-operation. (B) ANOVA of FoxP3<sup>+</sup> cell infiltration over time. Data are means ± SEM *n* = 4

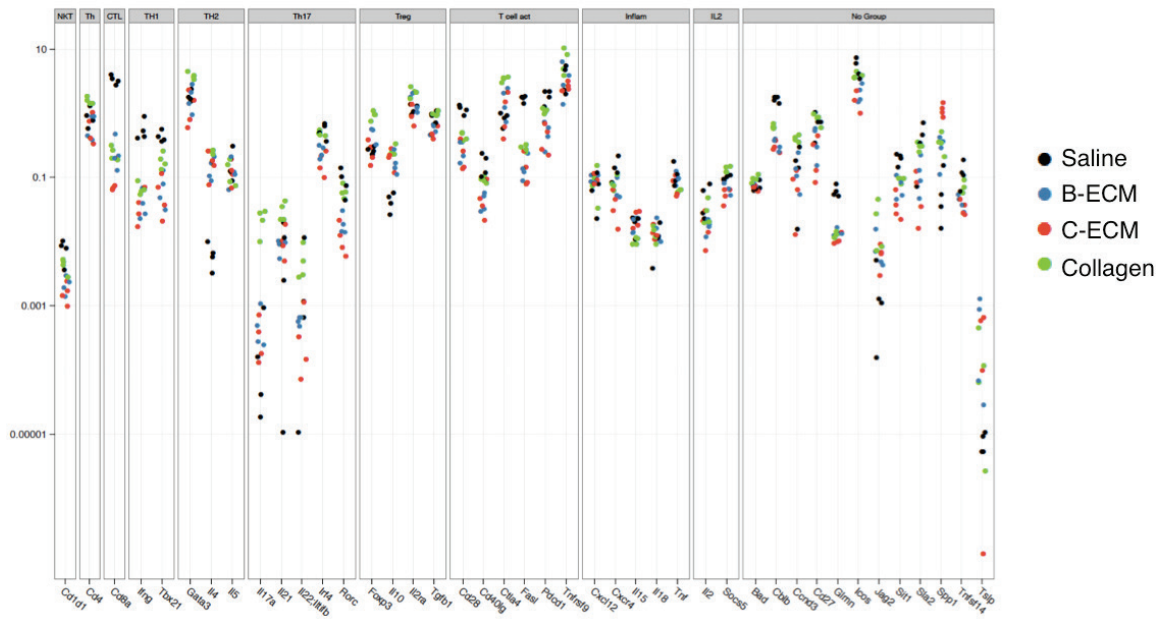


**Figure S4: Data spread of gene expression profiling of CD3<sup>+</sup> cells sorted from 1 week post surgery muscle defects. dCt of WT CD3<sup>+</sup> cells. Saline = Black dots. B-ECM = blue dots, C-ECM = red dots, Collagen = green dots.**

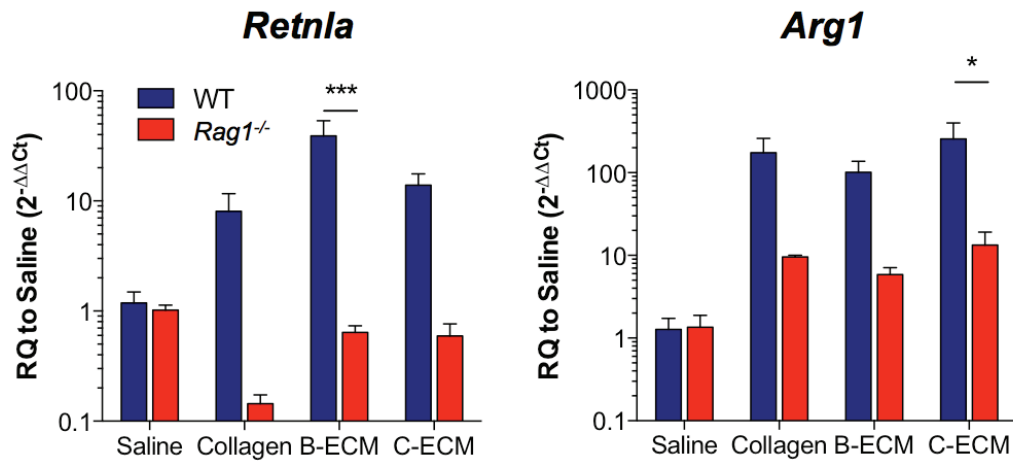


**Fig. S5: M2/M(IL4) Gene expression in scaffold-treated muscle wounds.** Biomaterial scaffolds induced the expression of two M2/M(IL4) myeloid genes, *Retnla*, encoding Fizz1 and *Arg1* encoding Arginase 1. ANOVA \*\*\* =  $P < 0.001$ , \* =  $P < 0.05$ . Data are means  $\pm$  SEM  $n = 4$ .

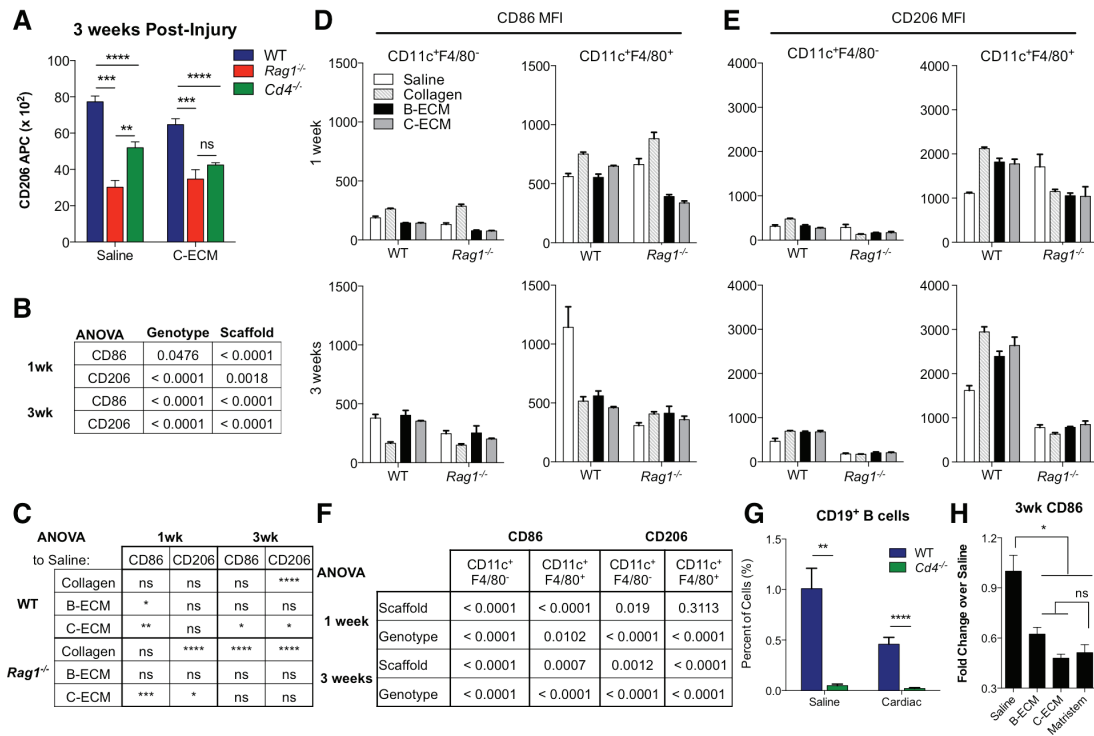


**Fig. S6: Myeloid polarization in WT, *Rag1*<sup>-/-</sup> and *Cd4*<sup>-/-</sup> mice.** (A) Confirmation of participation of CD4<sup>+</sup> T cells in M2-myeloid polarization as determined in *Rag1*<sup>-/-</sup> studies. CD206 mean fluorescence intensity in F4/80<sup>+</sup> macrophages from *Cd4*<sup>-/-</sup> mice compared to WT and *Rag1*<sup>-/-</sup> mice at 3wks post-injury. (B-E) Further analysis of WT versus *Rag1*<sup>-/-</sup> myeloid polarization. (B) Statistical analysis of overall effect of genotype and scaffold on expression of CD86 and CD206 at 1 and 3 weeks post surgery (C) Two-Way ANOVA comparing CD86 and CD206 expression in scaffold treatment to Saline control wounds at 1 and 3 weeks post surgery (D) Mean CD86 fluorescence intensity at 1 and 3 weeks post surgery in CD11c<sup>+</sup>F4/80<sup>-</sup> and CD11c<sup>+</sup>F4/80<sup>+</sup> dendritic cells. (E) Mean CD206 fluorescence intensity at 1 and 3 weeks post surgery in CD11c<sup>+</sup>F4/80<sup>-</sup> and CD11c<sup>+</sup>F4/80<sup>+</sup> dendritic cells (F) Two-way ANOVA of CD86 and CD206 expression at 1 and 3 weeks post surgery for CD11c<sup>+</sup>F4/80<sup>-</sup> and CD11c<sup>+</sup>F4/80<sup>+</sup> dendritic cells. (G) CD19<sup>+</sup> B cell recruitment, characteristic of Th2 phenotype, dependent on CD4<sup>+</sup> T cells. (H) B-ECM and C-ECM behave similarly to clinically used urinary-bladder matrix (UBM) material (Matristem). Decreased CD86 expression on F4/80<sup>+</sup> macrophages at 3 weeks post-injury in WT mouse displayed as fold change over Saline control. Data are means  $\pm$  SEM  $n = 4$ .

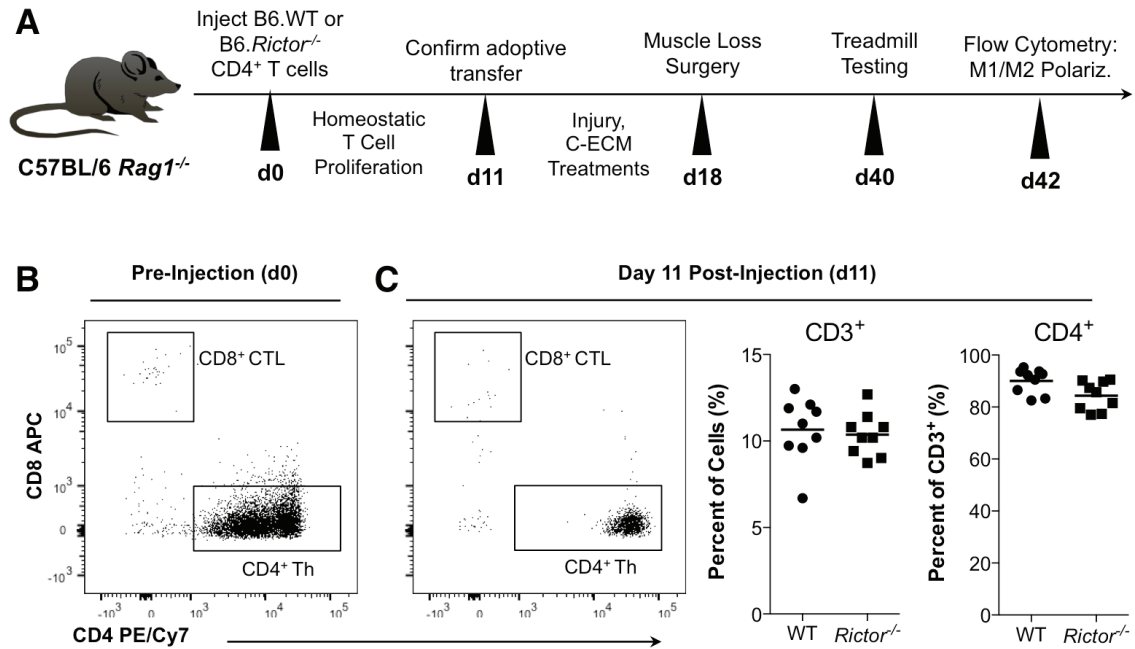


**Fig. S7: Adoptive Transfer of CD4<sup>+</sup> T cells into *Rag1*<sup>-/-</sup> mice.** (A) Timeline of adoptive transfer studies. (B) Purity confirmation of CD4<sup>+</sup> T cells after isolation from WT and *Rictor*<sup>F/F</sup> Cd4-Cre mice. (C) Confirmation of adoptive transfer at 11 days post-injection.

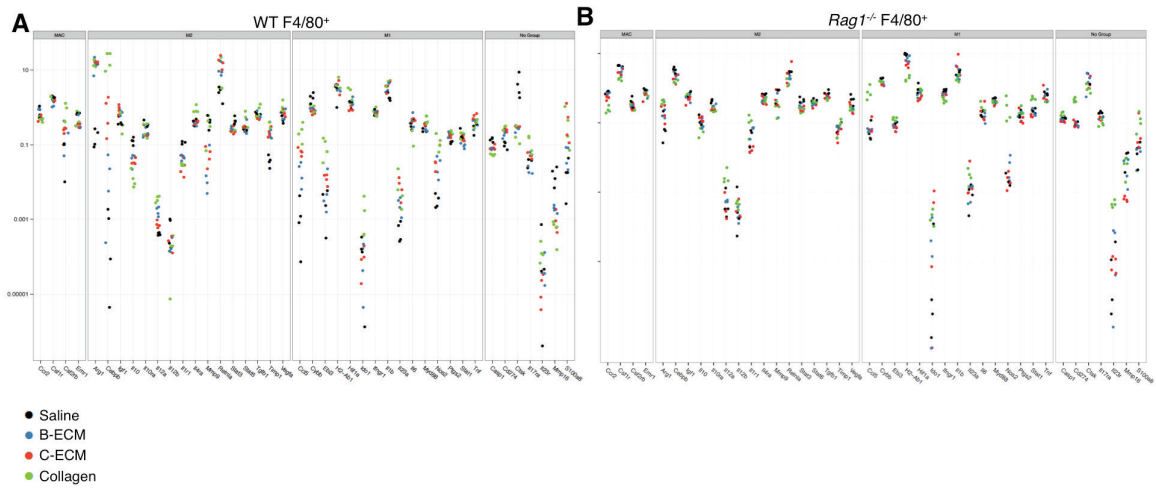


**Fig. S8: Data spread of gene expression profiling of cells sorted from 1 week post surgery muscle defects.** (A) dCt of WT F4/80<sup>+</sup> cells. (B) dCt of *Rag1*<sup>-/-</sup> F4/80<sup>+</sup> cells. Saline = black dots, Bone = blue, Cardiac = red, Collagen = green.

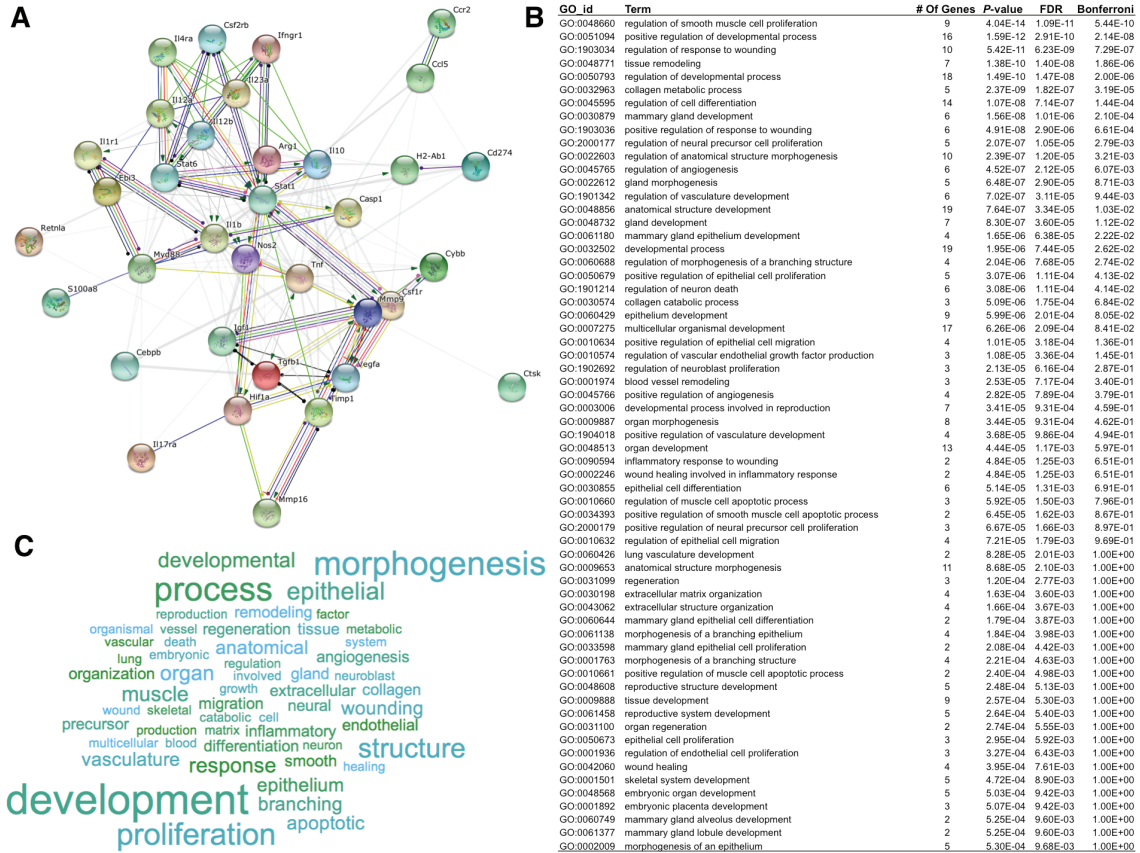


**Fig. S9: Gene ontology analysis of adaptive immune dependent gene expression changes in SIM F4/80<sup>+</sup> macrophages associated with wound healing and tissue regeneration.** Data displayed for genes significant in Fig. S7b (F4/80<sup>+</sup> Macrophages), input into STRING interaction database (35). (A) Gene interaction network. (B) GO processes that are significantly enriched (FDR  $P$ -value < 0.05) from genes that alter expression in *Rag1*<sup>-/-</sup> mice related to development and tissue regeneration. (C) Word map showing common terms in GO processes related to development and tissue regeneration.

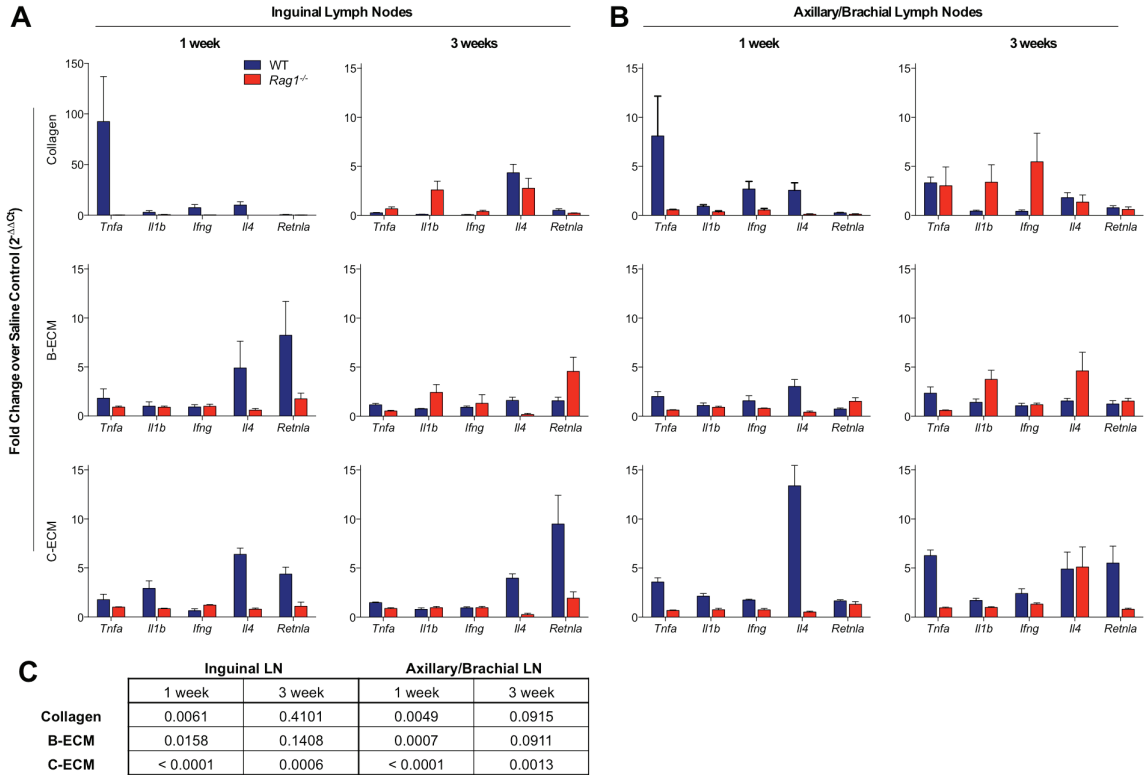


**Fig. S10: Gene expression in draining lymph nodes at 1 and 3 weeks post-operation.** Gene expression was measured in local (A, inguinal) and distal (B, axillary/brachial) lymph nodes at 1 and 3 weeks post-operation to measure type-1 (*Tnfa*, *Il1b*, *Ifng*) and type-2 (*Il4*, *Retnla*) gene changes dependent upon scaffold application. (C) ANOVA of WT versus *Rag1*<sup>-/-</sup> effect on gene expression. Data are means ± SEM. (*n* = 4, Saline, B-ECM, C-ECM; *n* = 3, collagen).



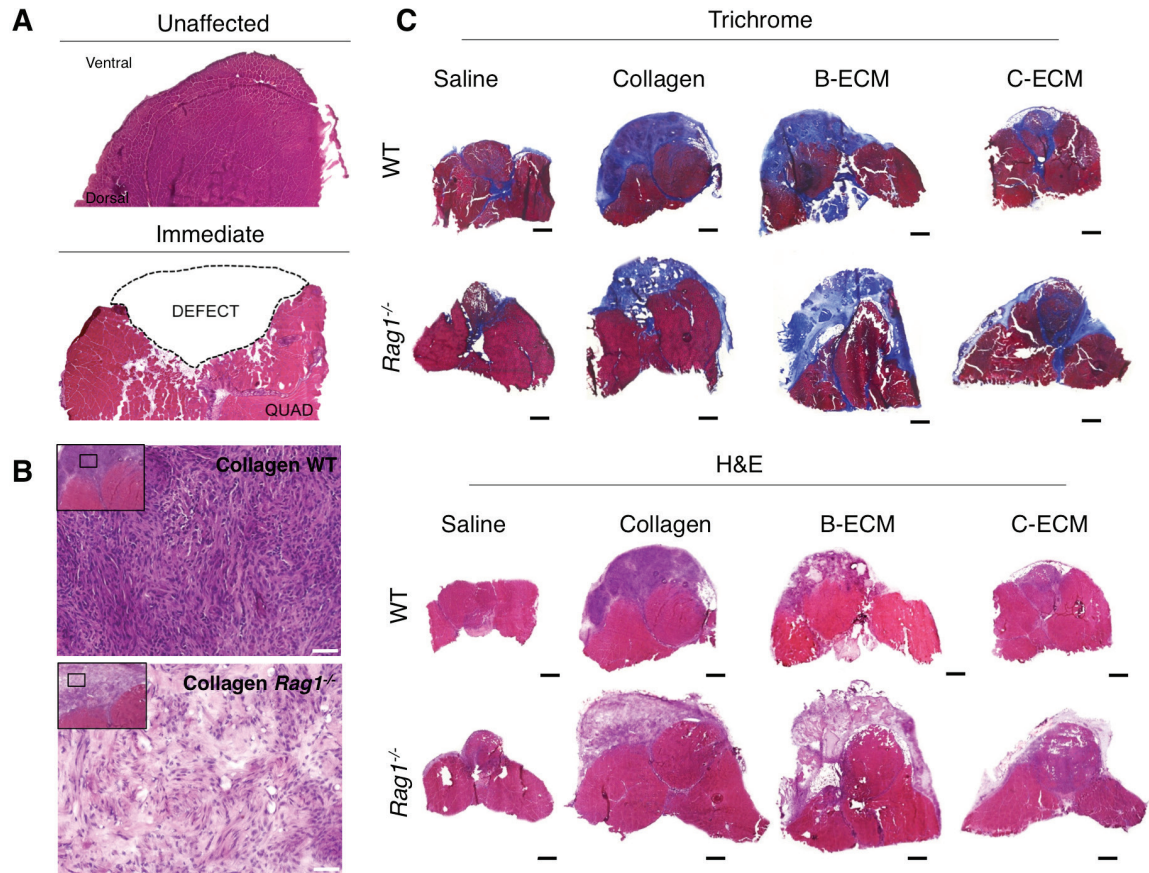


**Figure S12: Quadriceps muscle at 3 weeks post-operation in WT and *Rag1*<sup>-/-</sup> mice.** (A) Hematoxylin and eosin-stained histological sections of unaffected and affected quadriceps muscle immediately after volumetric muscle loss surgery. (B) Increased fibrosis and decreased cellularity in Collagen treated scaffolds in absence of adaptive immune cells (*Rag1*<sup>-/-</sup>) at 3 weeks post-injury. (C) Mosaic of quadriceps muscle at 3 weeks post-operation stained with Masson's trichrome (top) and Hematoxylin and Eosin (bottom). Scale bars = 50 microns in (b) and 500 microns in (c).

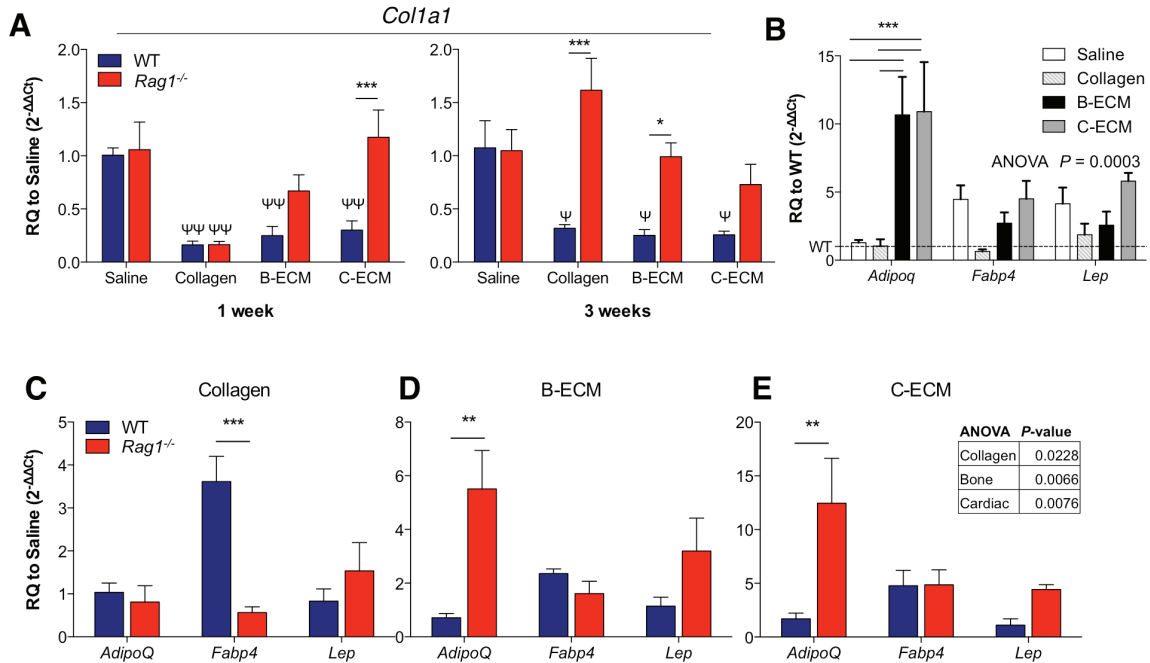


**Fig. S13: Collagen and adipose-related gene expression increases in *Rag1*<sup>-/-</sup> mice.** (A) *Col1a1* gene expression at 1 and 3 weeks post injury (B) Adipogenesis gene expression shown as a fold change over WT in corresponding scaffold treatment at 3 weeks post-injury (C-E) Adipogenesis gene expression displayed as a fold change over saline control in (C) collagen, (D) B-ECM and (E) C-ECM treated injuries at 3 weeks post-injury. Data are means  $\pm$  SEM  $n = 4$ . ANOVA \*\*\* =  $P < 0.001$ , \*\* =  $P < 0.01$ , \* =  $P < 0.05$  WT versus *Rag1*<sup>-/-</sup>. Panel A,  $\Psi$  = ANOVA vs Saline control.

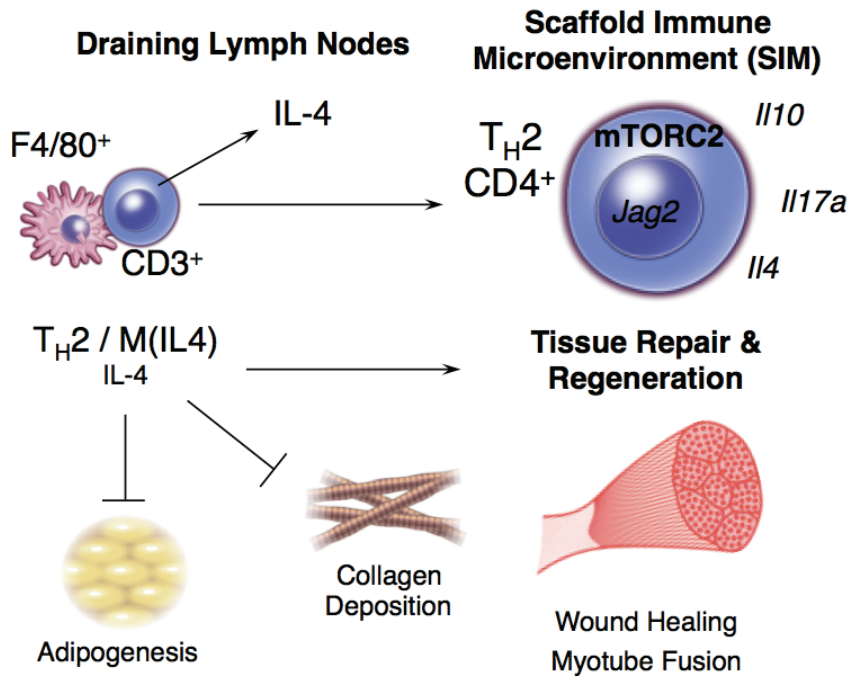


**Fig. S14: T cell participation in muscle regeneration and fibro/adipogenic lineage commitment.** T cell activation and polarization induce local Th2/M(IL-4) polarization of the SIM, promoting regenerative phenotypes such as wound healing and myotube fusion, and inhibit intramuscular adipose formation and collagen deposition. We hypothesize that the process begins with an innate response, in which ECM components induce a partial M2-like macrophage differentiation and simultaneously present ECM protein-derived peptides to T cells together with IL-4 production that drives Th2 differentiation. Th2 cells then significantly recruit and enhance M2 responses at the site of wound healing, forming a feed-forward amplification

**A**

Gene	Saline vs		
	B-ECM	C-ECM	Collagen
Cd1d1	0.029	0.029	0.200
Cd4	0.343	0.343	0.029
Cd8a	0.029	0.029	0.029
Ifng	0.029	0.029	0.029
Tbx21	0.029	0.029	0.029
Gata3	0.886	0.343	0.029
Il4	0.029	0.029	0.029
Il5	0.686	0.886	0.686
Il17a	0.200	0.486	0.029
Il21	1.000	0.886	0.029
Il22;Il1f1b	0.486	0.486	0.343
Irf4	0.029	0.029	0.486
Rorc	0.029	0.029	0.486
Foxp3	0.343	0.886	0.029
Il10	0.029	0.029	0.029
Il2ra	0.486	0.886	0.029
Tgfb1	0.029	0.029	1.000
Cd28	0.029	0.029	0.029
Cd40lg	0.029	0.029	0.029
Ctla4	0.200	0.886	0.029
Fasl	0.029	0.029	0.029
Pdcd1	0.029	0.029	0.029
Tnfrsf9	1.000	0.886	0.200
Cxcl12	0.343	0.486	0.686
Cxcr4	0.057	0.029	0.057
Il15	1.000	0.686	0.114
Il18	0.886	0.686	0.886
Tnf	1.000	0.200	0.029
Il2	0.029	0.114	0.343
Socs5	0.057	0.029	0.029
Bad	0.343	0.886	0.057
Cblb	0.029	0.029	0.029
Ccnd3	0.686	0.200	0.029
Cd27	0.114	0.057	0.686
Glmn	0.029	0.029	0.029
Icos	0.029	0.029	0.486
Jag2	0.114	0.057	0.029
Sit1	0.029	0.029	0.029
Sla2	0.200	0.114	0.486
Spp1	0.057	0.029	0.029
Tnfsf14	0.029	0.029	0.114
Tslp	0.029	0.309	0.309

**B**

Gene Group	Saline vs		
	B-ECM	C-ECM	Collagen
NKT	0.024	0.025	0.208
Th	0.328	0.35	0.023
CTL	0.024	0.025	0.023
Th1	0.024	0.025	0.023
Th2	0.087	0.079	0.057
Th17	0.12	0.12	0.112
Treg	0.075	0.085	0.048
T cell act	0.076	0.078	0.052
Inflamm	0.251	0.152	0.144
IL2	0.059	0.053	0.045

**Table S1. Wilcoxon Rank Sum Test Results on sorted CD3<sup>+</sup> T cells (A) CD3<sup>+</sup> Genes analyzed in scaffold treated vs. saline control. (B) CD3<sup>+</sup> gene group analysis.**

Gene	WT			<i>Rag1</i> <sup>-/-</sup>		
	Saline vs			Saline vs		
	B-ECM	C-ECM	Collagen	B-ECM	C-ECM	Collagen
Ccr2	1.000	0.343	0.057	0.686	0.029	0.343
Csf1r	0.029	0.114	0.886	0.029	0.114	0.057
Csf2rb	0.200	0.029	0.029	0.114	0.686	0.029
Emr1	0.057	0.029	0.886	0.343	1.000	0.886
Arg1	0.029	0.029	0.029	0.029	0.114	0.029
Cebpb	0.114	0.029	0.029	0.029	0.057	0.029
Igf1	0.029	0.029	1.000	0.343	0.029	0.343
Il10	0.029	0.029	0.029	0.029	0.200	0.029
Il10ra	0.029	0.029	0.686	0.114	0.686	0.057
Il12a	0.029	0.029	0.029	1.000	1.000	0.343
Il12b	0.114	0.486	0.343	0.029	0.114	1.000
Il1r1	0.057	0.029	0.029	0.343	0.343	0.029
Il4ra	0.200	0.886	0.029	0.886	0.486	0.029
Mmp9	0.029	0.029	0.686	0.686	0.114	0.886
Retnla	0.029	0.029	0.114	0.029	0.029	0.057
Stat3	0.029	0.029	0.200	0.029	0.114	0.029
Stat6	0.343	0.114	0.057	0.029	0.343	0.029
Tgfb1	1.000	0.057	1.000	0.886	0.486	0.114
Timp1	0.029	0.029	0.029	0.029	0.486	0.343
Vegfa	0.486	0.343	0.057	0.029	0.029	0.029
Ccl5	0.029	0.029	0.029	0.114	0.114	0.200
Cybb	0.029	0.029	0.029	0.029	0.200	0.029
Ebi3	0.686	0.029	0.029	0.029	0.486	0.029
H2-Ab1	1.000	0.200	0.200	1.000	0.486	0.886
Hif1a	0.886	0.057	0.114	0.029	1.000	0.486
Ido1	1.000	0.686	0.029	0.029	0.343	0.029
Ifngr1	0.486	0.686	1.000	0.886	0.114	0.029
Il1b	0.029	0.057	0.029	0.686	0.029	0.114
Il23a	0.029	0.029	0.029	0.029	0.029	0.057
Il6	0.486	0.114	0.686	0.029	0.029	0.029
Myd88	0.686	0.029	0.029	0.686	0.057	0.029
Nos2	0.029	0.029	0.029	0.029	0.343	0.200
Ptgs2	0.057	0.114	0.029	0.029	0.057	0.029
Stat1	0.029	0.114	0.886	0.029	0.057	0.029
Tnf	0.886	0.057	0.486	0.686	0.029	0.029
Casp1	0.029	0.029	0.029	0.029	0.029	0.029
Cd274	0.029	0.029	0.029	0.343	0.057	0.029
Ctsk	0.029	0.029	0.029	0.057	0.057	0.486
Il17ra	0.486	0.029	0.029	0.029	0.029	0.200
Il23r	0.686	0.343	0.343	0.029	0.029	0.029
Mmp16	0.029	0.029	0.029	0.029	0.057	0.029
S100a8	0.114	0.029	0.029	0.029	0.200	0.029

Gene	WT vs <i>Rag1</i> <sup>-/-</sup>		
	B-ECM	C-ECM	Collagen
Ccr2	0.71	0.843	0.002
Csf1r	0.991	0.111	<0.001
Csf2rb	0.023	0.004	<0.001
Arg1	<0.001	<0.001	<0.001
Cebpb	0.008	<0.001	<0.001
Igf1	0.007	<0.001	0.724
Il10	0.004	<0.001	<0.001
Il12a	0.021	0.12	0.568
Il12b	0.413	0.234	0.032
Il1r1	0.237	0.393	<0.001
Il4ra	0.131	0.022	<0.001
Mmp9	0.002	0.029	0.435
Retnla	0.001	<0.001	0.002
Stat6	0.289	0.051	0.008
Tgfb1	0.261	0.979	0.003
Timp1	<0.001	<0.001	<0.001
Vegfa	0.011	0.006	<0.001
Ccl5	<0.001	<0.001	<0.001
Cybb	0.021	0.004	0.005
Ebi3	0.142	0.008	<0.001
H2-Ab1	0.115	0.003	<0.001
Hif1a	0.071	0.211	0.003
Ifngr1	0.413	0.028	<0.001
Il1b	0.052	0.276	<0.001
Il23a	0.06	0.023	0.119
Myd88	0.021	<0.001	<0.001
Nos2	0.039	<0.001	0.08
Stat1	0.002	0.787	<0.001
Tnf	0.336	0.033	0.022
Casp1	<0.001	0.007	<0.001
Cd274	<0.001	<0.001	0.007
Ctsk	<0.001	<0.001	<0.001
Il17ra	0.775	0.022	<0.001
Mmp16	0.063	0.748	<0.001
S100a8	0.177	0.042	0.358

**Table S2. Wilcoxon Rank Sum and Linear Regression Test Results on sorted F4/80<sup>+</sup> macrophages in WT and *Rag1*<sup>-/-</sup> mice. (A) Wilcoxon Rank Sum test on F4/80<sup>+</sup> Genes analyzed in scaffold treated vs. saline control. (B) Linear Regression model on material by genotype interaction. WT vs. *Rag1*<sup>-/-</sup> comparison in effect of scaffold on gene expression changes versus saline treated control, p-values displayed for significant comparisons ( $P < 0.05$  in at least one scaffold treatments).**

## REFERENCES

1. T. A. Wynn, A. Chawla, J. W. Pollard, Macrophage biology in development, homeostasis and disease. *Nature* **496**, 445–455 (2013). [Medline doi:10.1038/nature12034](#)
2. P. Matzinger, T. Kamala, Tissue-based class control: The other side of tolerance. *Nat. Rev. Immunol.* **11**, 221–230 (2011). [Medline doi:10.1038/nri2940](#)
3. Y. Peng, D. A. Martin, J. Kenkel, K. Zhang, C. A. Ogden, K. B. Elkon, Innate and adaptive immune response to apoptotic cells. *J. Autoimmun.* **29**, 303–309 (2007). [Medline doi:10.1016/j.jaut.2007.07.017](#)
4. J. S. Otis, S. Niccoli, N. Hawdon, J. L. Sarvas, M. A. Frye, A. J. Chicco, S. J. Lees, Pro-inflammatory mediation of myoblast proliferation. *PLOS One* **9**, e92363 (2014). [Medline doi:10.1371/journal.pone.0092363](#)
5. S. Frantz, K. A. Vincent, O. Feron, R. A. Kelly, Innate immunity and angiogenesis. *Circ. Res.* **96**, 15–26 (2005). [Medline doi:10.1161/01.RES.0000153188.68898.ac](#)
6. J. M. Anderson, Biological responses to materials. *Annu. Rev. Mater. Res.* **31**, 81–110 (2001). [doi:10.1146/annurev.matsci.31.1.81](#)
7. J. M. Anderson, K. M. Miller, Biomaterial biocompatibility and the macrophage. *Biomaterials* **5**, 5–10 (1984). [Medline doi:10.1016/0142-9612\(84\)90060-7](#)
8. J. M. Anderson, Inflammatory response to implants. *ASAIO Trans.* **34**, 101–107 (1988). [Medline doi:10.1097/00002480-198804000-00005](#)
9. B. M. Sicari, J. P. Rubin, C. L. Dearth, M. T. Wolf, F. Ambrosio, M. Boninger, N. J. Turner, D. J. Weber, T. W. Simpson, A. Wyse, E. H. Brown, J. L. Dziki, L. E. Fisher, S. Brown, S. F. Badylak, An acellular biologic scaffold promotes skeletal muscle formation in mice and humans with volumetric muscle loss. *Sci. Transl. Med.* **6**, 234ra58 (2014). [Medline doi:10.1126/scitranslmed.3008085](#)
10. V. J. Mase Jr., J. R. Hsu, S. E. Wolf, J. C. Wenke, D. G. Baer, J. Owens, S. F. Badylak, T. J. Walters, Clinical application of an acellular biologic scaffold for surgical repair of a large, traumatic quadriceps femoris muscle defect. *Orthopedics* **33**, 511 (2010). [Medline](#)
11. B. N. Brown, R. Londono, S. Tottey, L. Zhang, K. A. Kukla, M. T. Wolf, K. A. Daly, J. E. Reing, S. F. Badylak, Macrophage phenotype as a predictor of constructive remodeling following the implantation of biologically derived surgical mesh materials. *Acta Biomater.* **8**, 978–987 (2012). [Medline doi:10.1016/j.actbio.2011.11.031](#)
12. B. M. Sicari, V. Agrawal, B. F. Siu, C. J. Medberry, C. L. Dearth, N. J. Turner, S. F. Badylak, A murine model of volumetric muscle loss and a regenerative medicine approach for tissue replacement. *Tissue Eng. Part A* **18**, 1941–1948 (2012). [Medline doi:10.1089/ten.tea.2012.0475](#)
13. V. Z. Beachley, M. T. Wolf, K. Sadtler, S. S. Manda, H. Jacobs, M. R. Blatchley, J. S. Bader, A. Pandey, D. Pardoll, J. H. Elisseeff, Tissue matrix arrays for high-throughput screening and systems analysis of cell function. *Nat. Methods* **12**, 1197–1204 (2015). [Medline doi:10.1038/nmeth.3619](#)

14. V. Salmon-Ehr, L. Ramont, G. Godeau, P. Birembaut, M. Guenounou, P. Bernard, F.-X. Maquart, Implication of interleukin-4 in wound healing. *Lab. Invest. J. Tech. Methods Pathol.* **80**, 1337–1343 (2000).
15. W. C. Gause, T. A. Wynn, J. E. Allen, Type 2 immunity and wound healing: Evolutionary refinement of adaptive immunity by helminths. *Nat. Rev. Immunol.* **13**, 607–614 (2013). [Medline doi:10.1038/nri3476](#)
16. J. E. Heredia, L. Mukundan, F. M. Chen, A. A. Mueller, R. C. Deo, R. M. Locksley, T. A. Rando, A. Chawla, Type 2 innate signals stimulate fibro/adipogenic progenitors to facilitate muscle regeneration. *Cell* **153**, 376–388 (2013). [Medline](#)
17. V. Horsley, K. M. Jansen, S. T. Mills, G. K. Pavlath, IL-4 acts as a myoblast recruitment factor during mammalian muscle growth. *Cell* **113**, 483–494 (2003). [Medline doi:10.1016/S0092-8674\(03\)00319-2](#)
18. T. C. Fang, Y. Yashiro-Ohtani, C. Del Bianco, D. M. Knoblock, S. C. Blacklow, W. S. Pear, Notch directly regulates Gata3 expression during T helper 2 cell differentiation. *Immunity* **27**, 100–110 (2007). [Medline doi:10.1016/j.immuni.2007.04.018](#)
19. P. J. Murray, J. E. Allen, S. K. Biswas, E. A. Fisher, D. W. Gilroy, S. Goerdts, S. Gordon, J. A. Hamilton, L. B. Ivashkiv, T. Lawrence, M. Locati, A. Mantovani, F. O. Martinez, J. L. Mege, D. M. Mosser, G. Natoli, J. P. Saeij, J. L. Schultze, K. A. Shirey, A. Sica, J. Suttles, I. Udalova, J. A. van Ginderachter, S. N. Vogel, T. A. Wynn, Macrophage activation and polarization: Nomenclature and experimental guidelines. *Immunity* **41**, 14–20 (2014). [Medline doi:10.1016/j.immuni.2014.06.008](#)
20. G. M. Delgoffe, K. N. Pollizzi, A. T. Waickman, E. Heikamp, D. J. Meyers, M. R. Horton, B. Xiao, P. F. Worley, J. D. Powell, The kinase mTOR regulates the differentiation of helper T cells through the selective activation of signaling by mTORC1 and mTORC2. *Nat. Immunol.* **12**, 295–303 (2011). [Medline doi:10.1038/ni.2005](#)
21. D. Ruffell, F. Mourkioti, A. Gambardella, P. Kirstetter, R. G. Lopez, N. Rosenthal, C. Nerlov, A CREB-C/EBPbeta cascade induces M2 macrophage-specific gene expression and promotes muscle injury repair. *Proc. Natl. Acad. Sci. U.S.A.* **106**, 17475–17480 (2009). [Medline doi:10.1073/pnas.0908641106](#)
22. J. Blackwell, L. W. Harries, L. C. Pilling, L. Ferrucci, A. Jones, D. Melzer, Changes in CEBPB expression in circulating leukocytes following eccentric elbow-flexion exercise. *J. Physiol. Sci.* **65**, 145–150 (2015). [Medline doi:10.1007/s12576-014-0350-7](#)
23. M. E. Davis, J. P. Gumucio, K. B. Sugg, A. Bedi, C. L. Mendias, MMP inhibition as a potential method to augment the healing of skeletal muscle and tendon extracellular matrix. *J. Appl. Physiol.* **115**, 884–891 (2013). [Medline doi:10.1152/jappphysiol.00137.2013](#)
24. F. Mourkioti, N. Rosenthal, IGF-1, inflammation and stem cells: Interactions during muscle regeneration. *Trends Immunol.* **26**, 535–542 (2005). [Medline doi:10.1016/j.it.2005.08.002](#)
25. A. Musarò, K. McCullagh, A. Paul, L. Houghton, G. Dobrowolny, M. Molinaro, E. R. Barton, H. L. Sweeney, N. Rosenthal, Localized Igf-1 transgene expression sustains hypertrophy and regeneration in senescent skeletal muscle. *Nat. Genet.* **27**, 195–200 (2001). [Medline doi:10.1038/84839](#)

26. J. P. Liu, J. Baker, A. S. Perkins, E. J. Robertson, A. Efstratiadis, Mice carrying null mutations of the genes encoding insulin-like growth factor I (Igf-1) and type 1 IGF receptor (Igf1r). *Cell* **75**, 59–72 (1993). [Medline](#)
27. N. Arsic, S. Zacchigna, L. Zentilin, G. Ramirez-Correa, L. Pattarini, A. Salvi, G. Sinagra, M. Giacca, Vascular endothelial growth factor stimulates skeletal muscle regeneration in vivo. *Molecular Therapy: J. Am. Soc. Gene Therapy* **10**, 844–854 (2004).
28. A. J. Allman, T. B. McPherson, S. F. Badylak, L. C. Merrill, B. Kallakury, C. Sheehan, R. H. Raeder, D. W. Metzger, Xenogeneic extracellular matrix grafts elicit a TH2-restricted immune response. *Transplantation* **71**, 1631–1640 (2001). [Medline](#)  
[doi:10.1097/00007890-200106150-00024](https://doi.org/10.1097/00007890-200106150-00024)
29. A. J. Allman, T. B. McPherson, L. C. Merrill, S. F. Badylak, D. W. Metzger, The Th2-restricted immune response to xenogeneic small intestinal submucosa does not influence systemic protective immunity to viral and bacterial pathogens. *Tissue Eng.* **8**, 53–62 (2002). [Medline](#) [doi:10.1089/107632702753503054](https://doi.org/10.1089/107632702753503054)
30. S. A. Rosenberg, J. C. Yang, N. P. Restifo, Cancer immunotherapy: Moving beyond current vaccines. *Nat. Med.* **10**, 909–915 (2004). [Medline](#) [doi:10.1038/nm1100](https://doi.org/10.1038/nm1100)
31. O. A. Ali, C. Verbeke, C. Johnson, R. W. Sands, S. A. Lewin, D. White, E. Doherty, G. Dranoff, D. J. Mooney, Identification of immune factors regulating antitumor immunity using polymeric vaccines with multiple adjuvants. *Cancer Res.* **74**, 1670–1681 (2014). [Medline](#) [doi:10.1158/0008-5472.CAN-13-0777](https://doi.org/10.1158/0008-5472.CAN-13-0777)
32. J. Kim, D. J. Mooney, In vivo modulation of dendritic cells by engineered materials: towards new cancer vaccines. *Nano Today* **6**, 466–477 (2011). [Medline](#)  
[doi:10.1016/j.nantod.2011.08.005](https://doi.org/10.1016/j.nantod.2011.08.005)
33. O. A. Ali, P. Tayalia, D. Shvartsman, S. Lewin, D. J. Mooney, Inflammatory cytokines presented from polymer matrices differentially generate and activate DCs in situ. *Adv. Funct. Mater.* **23**, 4621–4628 (2013). [Medline](#) [doi:10.1002/adfm.201203859](https://doi.org/10.1002/adfm.201203859)
34. M. L. Squadrito, C. Baer, F. Burdet, C. Maderna, G. D. Gilfillan, R. Lyle, M. Ibberson, M. De Palma, Endogenous RNAs modulate microRNA sorting to exosomes and transfer to acceptor cells. *Cell Rep.* **8**, 1432–1446 (2014). [Medline](#)
35. D. Szklarczyk, A. Franceschini, S. Wyder, K. Forslund, D. Heller, J. Huerta-Cepas, M. Simonovic, A. Roth, A. Santos, K. P. Tsafou, M. Kuhn, P. Bork, L. J. Jensen, C. von Mering, STRING v10: Protein-protein interaction networks, integrated over the tree of life. *Nucleic Acids Res.* **43**, D447–D452 (2015). [Medline](#) [doi:10.1093/nar/gku1003](https://doi.org/10.1093/nar/gku1003)